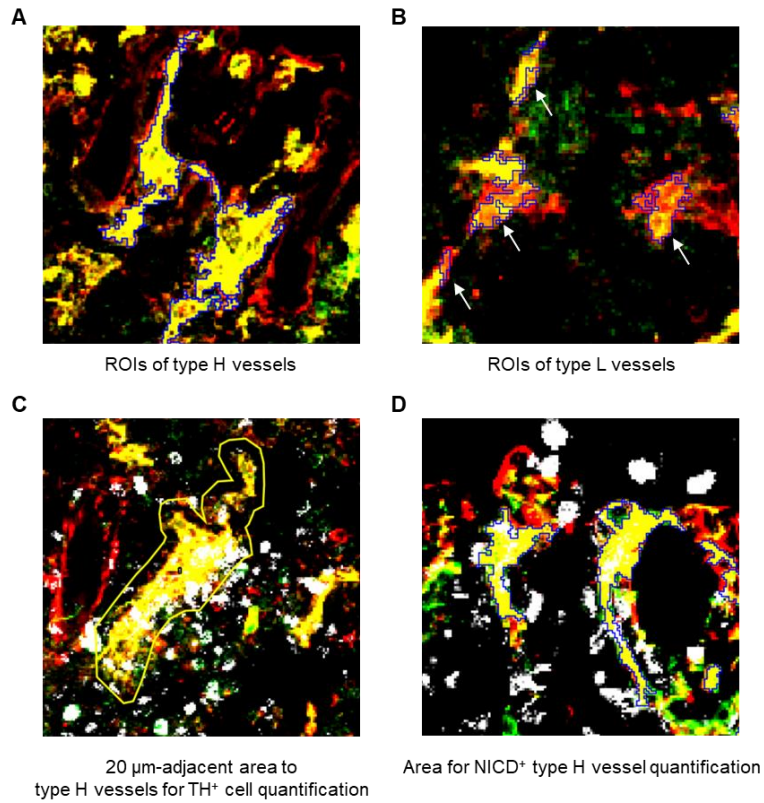


**Supplemental information**

**Region-specific sympatho-adrenergic  
regulation of specialized vasculature  
in bone homeostasis and regeneration**

**Hao-Kun Xu, Jie-Xi Liu, Chen-Xi Zheng, Lu Liu, Chao Ma, Jiong-Yi Tian, Yuan Yuan, Yuan Cao, Shu-Juan Xing, Si-Ying Liu, Qiang Li, Ya-Juan Zhao, Liang Kong, Yong-Jin Chen, and Bing-Dong Sui**

## Supplementary information



**Figure S1. Criteria for immunofluorescence quantification, related to STAR Methods.** (A) A representative of region of interest (ROI) of type H vessels (blue line). (B) A representative of ROI of type L vessels (blue line). (C) A representative of 20  $\mu\text{m}$ -adjacent area to type H vessels for TH<sup>+</sup> cell quantification. (D) A representative of area for NICD<sup>+</sup> type H vessel quantification.

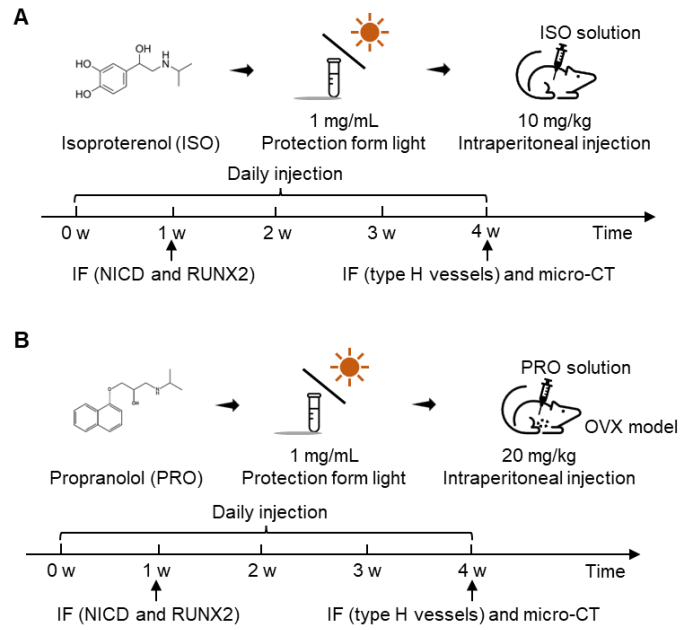


**Figure S2. Schematic diagram of mouse treatment, related to STAR Methods.** (A) Schematic diagram of ISO treatment, sample collection and examination of PBS and ISO groups. (B) Schematic diagram of PRO treatment and sample collection and examination of Sham, OVX and OVX+PRO groups.

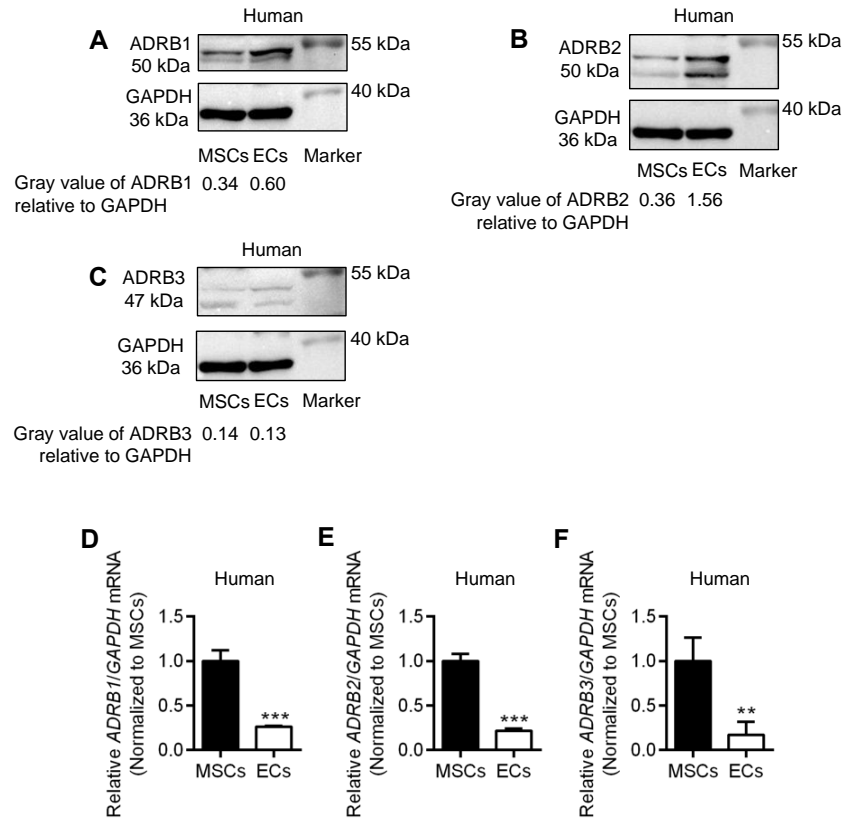


**Figure S3. Western blotting and qRT-PCR analysis of adrenergic receptors in human MSCs and ECs, related to Figure 1.** (A-C) Western blotting analysis of ADRB1/2/3 and GAPDH proteins in human-derived MSCs and ECs. (D and E) qRT-PCR analysis of *ADRB1/2/3* and *GAPDH* mRNA level in human-derived MSCs and ECs. Data represent mean  $\pm$  SD. Statistical analysis is performed by Student's *t* test. \*\*,  $P < 0.01$ ; \*\*\*,  $P < 0.001$ .

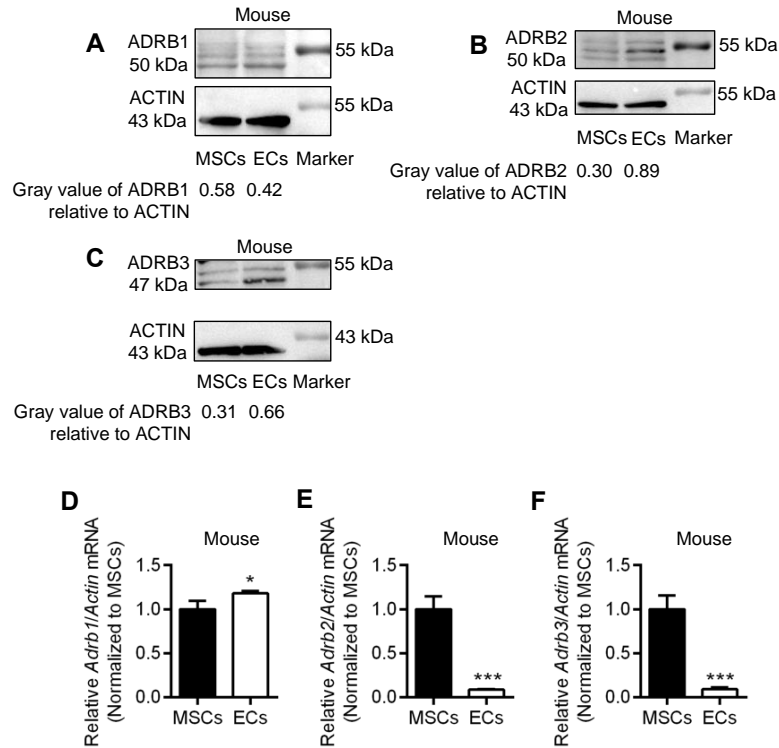


**Figure S4. Western blotting and qRT-PCR analysis of adrenergic receptors in mouse MSCs and ECs, related to Figure 1.** (A-C) Western blotting analysis of ADRB1/2/3 and ACTIN proteins in mouse-derived MSCs and ECs. (D and E) qRT-PCR analysis of *Adrb1/2/3* and *Actin* mRNA level in mouse-derived MSCs and ECs. Data represent mean  $\pm$  SD. Statistical analysis is performed by Student's *t* test. \*,  $P < 0.05$ ; \*\*\*,  $P < 0.001$ .

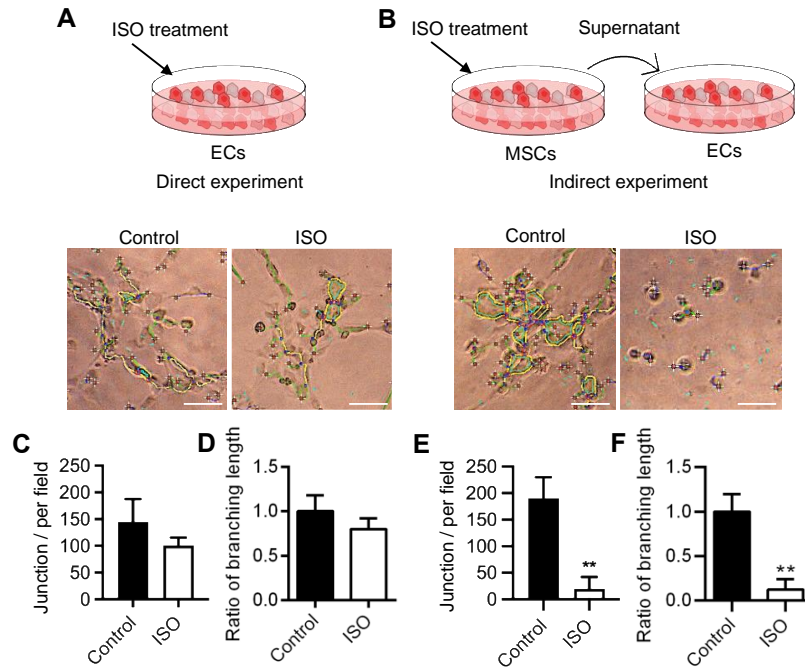


**Figure S5. Sympathoexcitation regulated angiogenesis of ECs through paracrine effects of MSCs, related to Figure 2.** (A) Schematic diagram and representative images of tube formation assay of human-derived ECs with ISO-direct treatment. Scale bar, 100  $\mu\text{m}$ . (B) Schematic diagram and representative images of tube formation assay of ECs with ISO-indirect treatment *via* MSCs. Human-derived MSCs and ECs were used Scale bar, 100  $\mu\text{m}$ . (C and D) Quantification of junction/per field and Ratio of branching length.  $N = 3$  per group. (E and F) Quantification of junction/per field and Ratio of branching length.  $N = 3$  per group. Data represent mean  $\pm$  SD. Statistical analysis is performed by Student's  $t$  test. \*\*,  $P < 0.01$ .

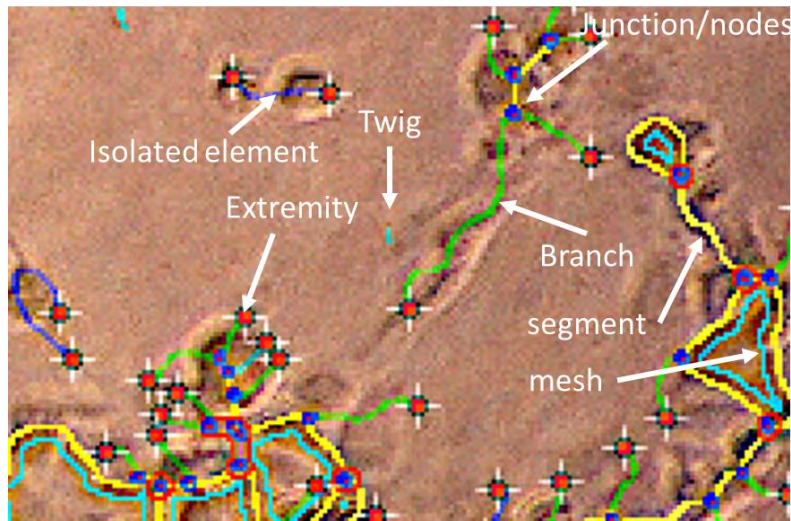


**Figure S6. Elements in the results of angiogenesis analyzer for ImageJ, related to STAR Methods.**

Segments are elements delimited by two junctions. Branches are elements delimited by a junction and one extremity. A twig is a branch whose size is lower than a user defined threshold value. Isolated elements are binary lines which are not branched. Meshes are areas enclosed by segments or master segments. Nodes refer to pixels with three neighboring pixels, typically forming a triangular pattern. Junctions are points in the image that can be identified as either individual nodes or clusters of fused nodes. Information can be found at URL of Angiogenesis Analyzer for ImageJ: <http://image.bio.methods.free.fr/ImageJ/?Angiogenesis-Analyzer-for-ImageJ&artpage=3-6&lang=en>).

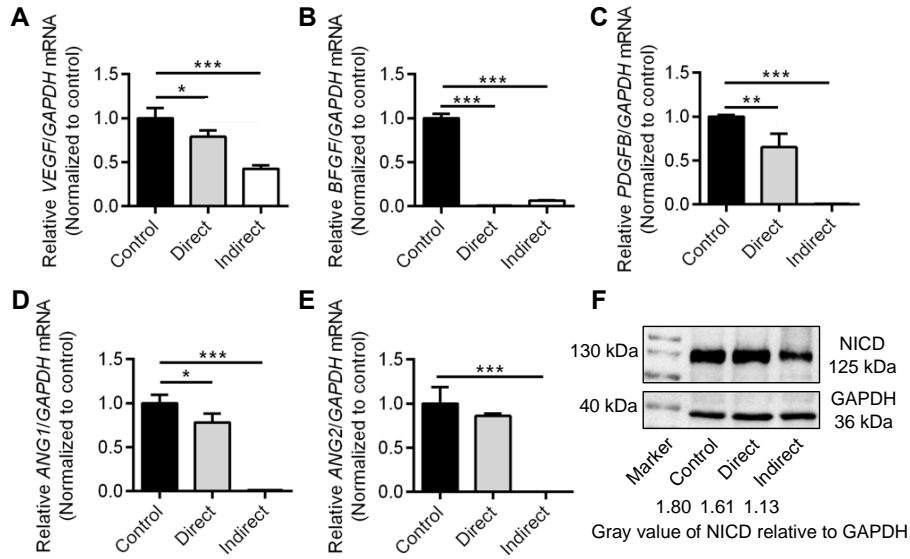


**Figure S7. qRT-PCR and western blotting analysis of angiogenic factors, related to Figure 2.** (A-E) qRT-PCR analysis of *VEGF*, *BFGF*, *PDGFB*, *ANG1*, *ANG2* and *GAPDH* mRNA level in human ECs. (F) Western blotting analysis of NICD and GAPDH proteins in ECs. Data represent mean  $\pm$  SD. Statistical analysis is performed by Student's *t* test for two-group comparison or by one-way analysis of variation followed by Newman-Keuls post-hoc tests for multiple comparisons. \*,  $P < 0.05$ ; \*\*,  $P < 0.01$ ; \*\*\*,  $P < 0.001$ .



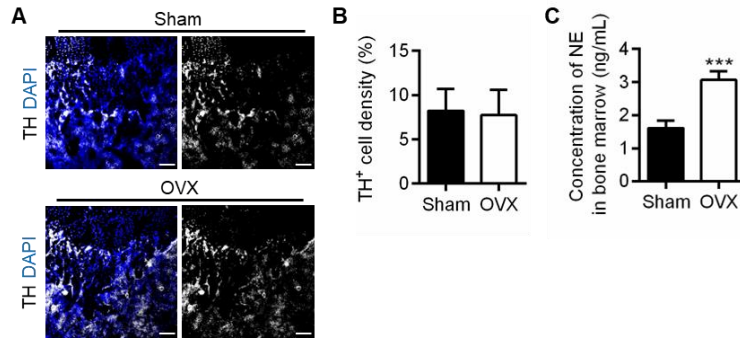


**Figure S8. Detection of TH<sup>+</sup> cell and NE level in bone, related to Figure 6.** (A) RUNX2 (white) immunostaining at metaphysis in femurs, counterstained by DAPI (blue). Dashed lines indicate the margin of growth plates. Scale bars, 100  $\mu$ m. (B) Quantification of TH<sup>+</sup> cell density (%).  $N = 3$  per group. (C) Concentration of NE in bone marrow.  $N = 3$  per group. Data represent mean  $\pm$  SD. Statistical analysis is performed by Student's  $t$  test. \*\*\*,  $P < 0.001$ .

**Table S1. List of sequences of primers used in this study, related to STAR Methods.**

<b>Mouse genes</b>	<b>Primer sequences</b>
<i>h-ADRB1</i>	Forward: 5'-ATCGAGACCCTGTGTGTCATT-3' Reverse: 5'-GTAGAAGGAGACTACGGACGAG-3'
<i>h-ADRB2</i>	Forward: 5'-TTGCTGGCACCCAATAGAAGC-3' Reverse: 5'-CAGACGCTCGAACTTGGCA-3'
<i>h-ADRB3</i>	Forward: 5'-GACCAACGTGTTTCGTGACTTC-3' Reverse: 5'-GCACAGGGTTTCGATGCTG-3'
<i>h-GAPDH</i>	Forward: 5'-GGAGCGAGATCCCTCCAAAAT-3' Reverse: 5'-GGCTGTTGTCATACTTCTCATGG-3'
<i>m-Adrb1</i>	Forward: 5'-CTCATCGTGGTGGGTAACGTG-3' Reverse: 5'-ACACACAGCACATCTACCGAA-3'
<i>m-Adrb2</i>	Forward: 5'-ATGTCGGTTATCGTCCTGGC-3' Reverse: 5'-GGTTTGTAGTCGCTCGAACTTG-3'
<i>m-Adrb3</i>	Forward: 5'-TCTCTGGCTTTGTGGTCGGA-3' Reverse: 5'-GTTGGTTATGGTCTGTAGTCTCG-3'
<i>m-Actb</i>	Forward: 5'-AGCGGTTCCGATGCCCT-3' Reverse: 5'-TTGGCATAGAGGTCTTTACGGATG-3'
<i>h-VEGF</i>	Forward: 5'-AGGGCAGAATCATCACGAAGT-3' Reverse: 5'-AGGGTCTCGATTGGATGGCA-3'
<i>h-BFGF</i>	Forward: 5'-AGTGTGTGCTAACCGTTACCT-3' Reverse: 5'-ACTGCCCAGTTCGTTTCAGTG-3'
<i>h-PDGFB</i>	Forward: 5'-CTCGATCCGCTCCTTTGATGA-3' Reverse: 5'-CGTTGGTGCGGTCTATGAG-3'
<i>h-ANG1</i>	Forward: 5'-AGCGCCGAAGTCCAGAAAAC-3' Reverse: 5'-TACTCTCACGACAGTTGCCAT-3'
<i>h-ANG2</i>	Forward: 5'-AACTTTCGGAAGAGCATGGAC-3' Reverse: 5'-CGAGTCATCGTATTCGAGCGG-3'